

Vortex currents and magnetic forces of non-magnetic plate in the process of magneto-pulse treatment on the ideal ferromagnetic platform

Abstract. Transients of medium current density and magnetic force in the weld volume with and without a ferromagnetic platform have been studied. The dependence of the amplitude values of the average current density and magnetic forces in the weld volume on the depth of penetration of the electromagnetic field through the non-magnetic plate for different variants of the plate thickness was studied.

Streszczenie. Zbadano przebiegi przejściowe średniej gęstości prądu i siły magnetycznej w objętości spoiny z platformą ferromagnetyczną i bez niej. Badano zależność wartości amplitud średniej gęstości prądu i sił magnetycznych w objętości spoiny od głębokości wnikania pola elektromagnetycznego przez płytę niemagnetyczną dla różnych wariantów grubości płyty. (Prądy wirkowe i siły magnetyczne płyty niemagnetycznej w procesie obróbki magneto-impulsowej na idealnej platformie ferromagnetycznej)

Keywords: magnetic pulse processing, U-shaped magnetic conductor, pulsed current, magnetic forces, ferromagnetic platform.

Słowa kluczowe: przetwarzanie impulsów magnetycznych, przewodnik magnetyczny w kształcie litery U, prąd pulsacyjny.

Introduction

The action of a pulsed current with a density of more than 10^6 A/m² with a pulse duration 10^{-4} ... 10^{-3} s leads to an electroplastic effect in metal products [1–3, 4, 5]. The electroplastic effect is manifested in the form of reduction of residual stresses, which is relevant for welds of metal structures. The electromagnetic field affects all structural levels: micro-, macro-, meso- and in almost all cases the end result is the result of the combined action of many of the above effects that occur at different levels of material structure. [1]. The macroscopic effects of the electromagnetic field are the result of its action on all structural and hierarchical levels of the material. Electromagnetic field causes a change in the properties of materials of different magnetic nature, which allows you to modify both magnetic and non-magnetic materials [2]. In [3] it was found that as a result of electrodynamic treatment of weld metal (butt weld) of G8A/GM70B alloy the number of cycles to the destruction of the samples in the case of symmetrical bending increases almost twice compared to untreated.

For local flow in the welds of non-magnetic pulse current plates, magnetic pulse treatment using pulsed electromagnetic field inductors is proposed. [6-8]. Such inductors can be with or without a magnetic circuit. The magnetic circuit allows you to achieve the desired pulsed eddy current with lower requirements for the power supply - less current and voltage in the inductor winding [9].

In fig. 1 shows a sketch of the induction system. The flow of pulsed current in the winding of the inductor 2 with U-shaped magnetic circuit 1 induces eddy currents in the non-magnetic plate 3. Placing a non-magnetic plate 3 with a weld on the ferromagnetic platform 4 can allow to concentrate the magnetic field in the area eddy current and magnetic forces in the weld [13]. The depth of penetration of the electromagnetic field δ in the non-magnetic plate 3 depends on the duration of the current pulse T_i and electrical conductivity σ of the plate. The current frequency F is used to estimate the depth of penetration of the electromagnetic field through the nonmagnetic plate A. To estimate the depth of penetration of the electromagnetic

field through the non-magnetic plate δ , the current frequency f is used, the period of which corresponds to twice the pulse duration $2T_i$. It is known that if the depth of penetration δ of the electromagnetic field into the plate is less than its thickness g , the presence of a ferromagnetic platform will not have a significant effect on the distribution of the electromagnetic field in the plate. [13].

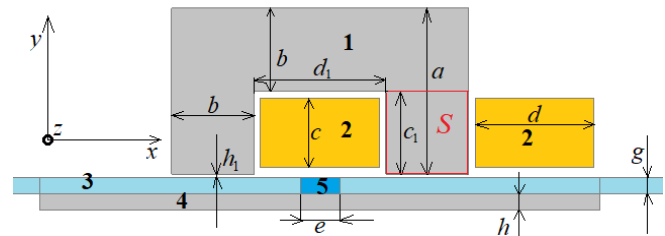


Fig. 1. Sketch of the induction system

The aim of the work is to determine the effect of electromagnetic field permeability through non-magnetic plates with welded joints of different thickness, placed on a ferromagnetic platform, on the current density and magnetic forces in the volume of welds.

The ferromagnetic platform can enter a saturated state in the process of current pulse in the inductor winding, and the currents in the inductor winding will change with changing parameters of the non-magnetic plate. Therefore, it is proposed to study the effect of non-magnetic plate parameters and the presence of a ferromagnetic platform on currents and magnetic forces in the weld of a non-magnetic plate with the same conditions: the parameters of the ferromagnetic platform μ , σ – const; pulsed current in the winding $i(t)$ – const.

Magnetic field equation. To achieve the goal of the work, numerical modeling by the finite element method is used. Maxwell's equations, material equations and equations for vector magnetic potential are used to calculate the electromagnetic fields of the electromagnetic system:

$$(1) \quad \operatorname{div} \mathbf{B} = 0, \quad \operatorname{rot} \mathbf{E} = -\partial \mathbf{B} / \partial t, \quad \operatorname{rot} \mathbf{H} = \mathbf{j}, \quad \mathbf{B} = \mu \mathbf{H}, \\ \mathbf{j} = \sigma \mathbf{E} + \mathbf{j}_s, \quad \operatorname{rot} \mathbf{A} = \mathbf{B}, \quad \mathbf{E} = -\partial \mathbf{A} / \partial t,$$

where \mathbf{H} , \mathbf{j} , \mathbf{A} , \mathbf{B} , \mathbf{E} , \mathbf{j}_s – respectively vectors of magnetic field strength, current density, vector magnetic potential, magnetic field induction, electric field strength, current density of the power supply, t – time. Based on (1), the following magnetic field equation for the vector magnetic potential is obtained [10]:

$$(2) \quad \operatorname{rot}(\operatorname{rot} \mathbf{A} / \mu) = -\sigma \partial \mathbf{A} / \partial t + \mathbf{j}_s.$$

In the model in the two-dimensional formulation of the induction system there is only component A_z of the vector magnetic potential (fig. 1). Therefore, equation 2 has the form:

$$(3) \quad \operatorname{rot}_z(\operatorname{rot}(\bar{z}A_z) / \mu) = -\sigma \partial A_z / \partial t + j_{sz}$$

where \bar{z} – unit vector in the z coordinate. The current density of the power supply j_{sz} , which is present in areas 2 (Fig. 1)

$$(4) \quad j_{sz} = \zeta \frac{i(t)}{s_w k_a}, \quad \text{where } k_a = \frac{s_a}{s_w N_w}, \quad s_a = c \cdot d$$

ζ – polarity of current in the cross section of the winding 2 (Fig. 1), $i(t)$ – current function depending on time, s_w – cross section of one winding conductor, k_a – the ratio of the cross section s_a of the winding area 2 (Fig. 1) to the total cross section of the conductors in this area, N_w – the number of cross sections of the turns of the winding 2 (Fig. 1).

The magnetic field equation (3) taking into account (4) is written as follows:

$$(5) \quad \operatorname{rot}_z \left(\frac{\operatorname{rot}(\bar{z}A_z)}{\mu} \right) + \sigma \frac{\partial A_z}{\partial t} = \zeta \frac{i(t) N_w}{s_a}$$

The equation of an electric circuit. The induction system (fig. 1) is powered from a charged to a certain voltage capacitor. The electric circuit (Fig. 2, a) consists of a capacitor, inductance and active resistance.

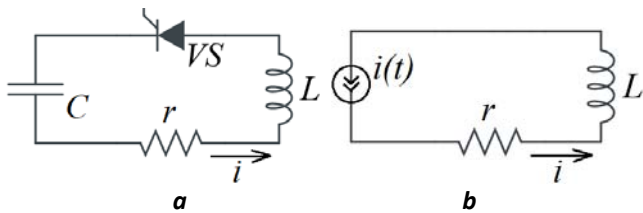


Fig. 2. Electric circuit

The equation according to Kirchhoff's second law has the form [11]

$$(6) \quad \frac{\partial \psi}{\partial t} + ri + \frac{1}{C} \int_0^t i dt + u_c(t=0) = 0$$

here ψ – flow coupling, determined from the solution of equation (5) for each moment of the discrete time interval $t = t_1, t_2, \dots, t_3$ c, i – instantaneous value of current in the

conductors of an electrical circuit, r – active resistance of a direct current in an electric circuit, C – capacitor capacity, $u_c(t)$ – capacitor voltage at time $t = 0$.

Because the thyristor is used in the circuit, after the first half of the oscillation period, the electrical circuit opens and the current remains zero. Taking into account the flux coupling ψ from the solution of equation (6), the equation of the electric circuit (7) has the form:

$$(7) \quad \zeta \frac{N_w l'}{s_a} \int_{s_a} \frac{\partial A_z}{\partial t} ds_a + ri + \frac{1}{C} \int_0^t i dt = -u_c(t=0)$$

here l' – the depth of the model (Fig. 1) on the z coordinate, which must be set to determine the flow coupling.

Model for research

The calculation of the current $i(t)$ in the inductor winding is performed by a numerical method with the joint solution of the equations of the magnetic field (5) and the electric circuit (7) for moments of time $t = 0, 20, \dots, 1000$ mcs. Fig. 1 is used to model the electromagnetic field of the induction system by finite element in two-dimensional formulation. 2, a is a diagram for calculating the current $i(t)$. How the parameters of the model in two-dimensional formulation differ from the parameters in three-dimensional formulation is a study in [7]. The magnetic circuit 1 has a nonlinear parameter of magnetic permeability $\mu(\mathbf{B})$, electrical conductivity of the magnetic circuit $\sigma = 0$ Sm/m. Areas 2 of the cross section of the winding are continuous and current flows in them j_{sz} (4). Ferromagnetic platform 4: $\mu = \mu_r \mu_0 = 1000 \mu_0$, where μ_r – relative magnetic permeability, and electrical conductivity $\sigma = 0$ Sm/m. Electrical conductivity of a nonmagnetic plate $\sigma = 50 \times 10^6$ Sm/m. The following parameters of the electrical circuit are set (fig. 2, a): capacitor capacity – $C = 2$ mF, the voltage of the charged capacitor at the initial time – $u_c(0) = 800$ V, active resistance $r = 0,008$ Ohm, $N_w = 36$ cross sections of turns (18 turns in the coil). Dimensions of the model (fig. 1): $a = 50$ mm, $b = 25$ mm, $c = 21$ mm, $d = 36$ mm, $e = 12$ mm, $g = 5$ mm, $h = 5$ mm, $h_1 = 0,5$ mm, $c_1 = 25$ mm, $d_1 = 40$ mm, $l' = 100$ mm.

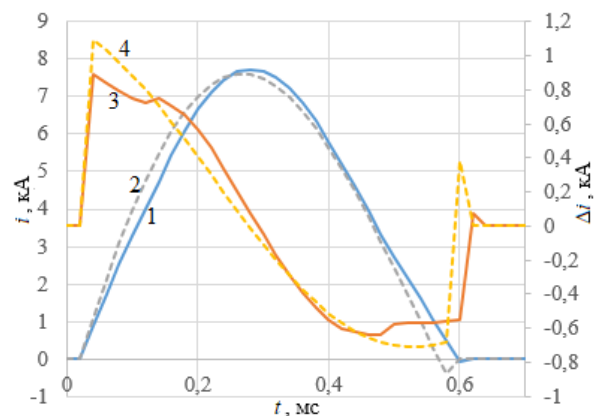


Fig. 3. Current function

As a result in fig. 3 (curve 1) the current function as a function of time is obtained $i(t)$, the duration of which is 600 mcs, and the acceleration of the function $\Delta i(\Delta t)$ for time intervals $\Delta t = 20$ mcs (fig. 3 – curve 3).

The acceleration of the function (curve 3) changes nonlinearly over time 0,05...0,2 ms and 0,4...0,55 ms due to the transition of the tooth of the magnetic circuit covered by the winding from unsaturated to saturated. The average value of induction in the tooth of the magnetic circuit with an area S (fig. 1) at the time $t = 280$ mcs (fig. 3, curve 1), when the current $i(t)$ is maximum is:

$$(8) \quad |\mathbf{B}|_{av} = \frac{1}{S} \int \text{rot} \mathbf{A} dS = 2,62 \text{ T}$$

The magnetic field strength is approximately $3,3 \cdot 10^5$ A/m for induction 2,62 T (magnetization curve of steel grade 2013). Therefore, the magnetic permeability of the saturated tooth of the magnetic circuit $\mu \approx 6,3 \mu_0$.

To compare the current function taking into account and without taking into account the magnetization curve of the magnetic circuit, the simulation of the current distribution over time with a constant magnetic permeability of the magnetic circuit is performed $\mu = 6,3 \mu_0$ (fig. 3, curve 2), and the acceleration of this function $\Delta i(\Delta t)$ for time intervals $\Delta t = 20$ mcs (fig. 3 – curve 4) is obtained. From fig. 3 shows that without taking into account the magnetization curve of the magnetic circuit, the acceleration of the current in time (curve 4) changes linearly over time 0,05...0,2 ms and 0,4...0,55 ms, compared to curve 3. Current curves 1 and 2 are similar, with a difference in amplitude values of 2%.

To establish the effect of electromagnetic field permeability δ through non-magnetic plates of different thickness g , placed on a ferromagnetic platform on the current density and magnetic forces in the volume of welds of these plates $i(t)$, which in fig. 3 (curve 1), and electrical conductivity σ of the nonmagnetic plate in table 1. Electromagnetic field permeability δ in table 1 is calculated using the current frequency f , corresponding to the period $2T_i = 1,2$ ms (fig. 3, curve 1).

The electric circuit used in fig. 2, b, in which current source $i(t)$ is curve 1 in fig. 4. Calculation of the average amplitude value of the current density j_{av} and bulk density of magnetic force F_{av} is performed by expressions:

$$(9) \quad j_{av} = \frac{1}{S} \int \left| \text{rot}_z \left(\frac{\text{rot}(\vec{z} A_z)}{\mu} \right) \right| dS$$

σ , MSm/m	304,09	76,02	33,79	19,01	12,16	8,45	6,21	4,75	3,75	3,04
δ , mm	1	2	3	4	5	6	7	8	9	10

$$(10) \quad F_{av} = \frac{1}{S} \int \sqrt{\left(\frac{\partial T_{xx}}{\partial x} + \frac{\partial T_{xy}}{\partial y} \right)^2 + \left(\frac{\partial T_{yx}}{\partial x} + \frac{\partial T_{yy}}{\partial y} \right)^2} dS$$

in which \mathbf{S} is the area of the weld 5 (fig. 2, 3), \mathbf{T} is the tension tensor of the magnetic force [11]

$$(11) \quad \mathbf{T} = \frac{1}{\mu} \begin{bmatrix} B_x^2 - B^2/2 & B_x B_y \\ B_x B_y & B_y^2 - B^2/2 \end{bmatrix}$$

Research results.

In fig. 4 shows the current density (9) at the corresponding values σ and δ (table 1) of the plate, the thickness $g = 5$ mm: a – without ferromagnetic platform, b – with ferromagnetic platform. With a decrease in the electrical conductivity of the nonmagnetic plate, and an increase in the depth of penetration of the electromagnetic field through the plate (table 1), we have a decrease in the current density. It is seen that the current density depends inversely proportional to the depth of penetration δ – per millimeter δ the current density varies by almost the same amount. Using a ferromagnetic platform (fig. 4, b), the current density is higher than without the platform (fig. 4, a). At the end of the current pulse 0,6 ms (fig. 3, curve 1) the current density has a second maximum (fig. 4) with opposite polarity along the axis z [8]. And this maximum is much higher at $\delta < g$ (fig. 4). If the depth of permeability of the magnetic field is equal to the thickness of the non-magnetic plate $\delta = g$, then there is up to 50% less current density at time 0,6 ms with the presence of a ferromagnetic platform. Provided that $\delta > g$ the presence of a ferromagnetic platform allows to reduce by 2 times the maximum current at a time of 0,6 ms and thus obtain a more unipolar current in a non-magnetic plate.

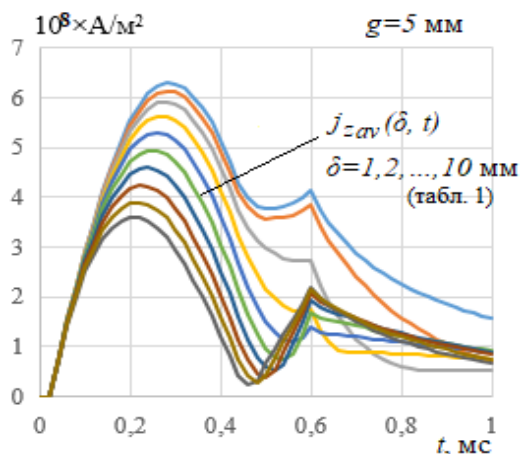


Fig. 4.a. Current density without ferromagnetic platform

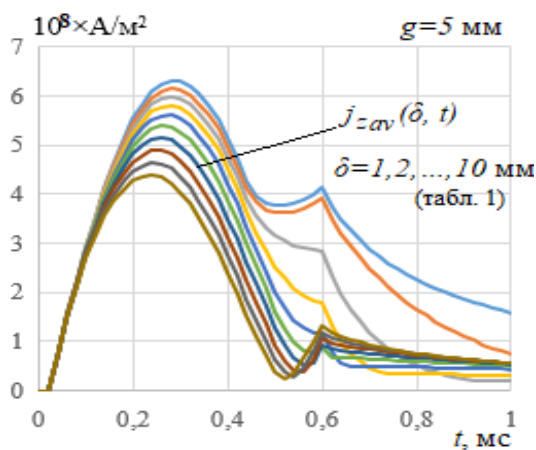


Fig. 4.b. Current density with ferromagnetic platform

In fig. 5, 6, 7 show the dependence of the amplitude values of current (9) and magnetic force (10) on the depth of penetration of the electromagnetic field δ in accordance with the thickness of the plate $g=1, 5, 10$ mm. Symbols used: 1 and 2 - current density, respectively, without ferromagnetic platform and with the platform; 3 and 4 - magnetic force density, respectively, without ferromagnetic platform and with the platform; 5 - the ratio of the current density with the platform to the current density without the platform; 6 - the ratio of the magnetic force density with a platform to the magnetic force density without a platform.

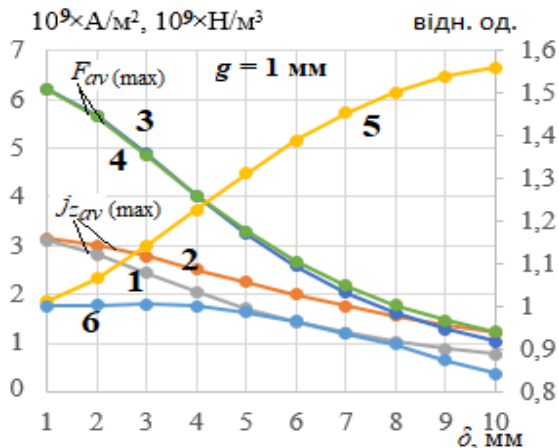


Fig. 5. Current and magnetic force on the depth of penetration of the electromagnetic field δ in accordance with the thickness of the plate $g=1$ mm.

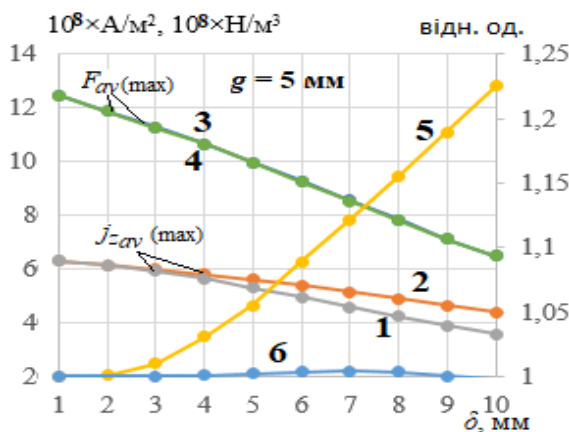


Fig. 6. Current and magnetic force on the depth of penetration of the electromagnetic field δ in accordance with the thickness of the plate $g=5$ mm.

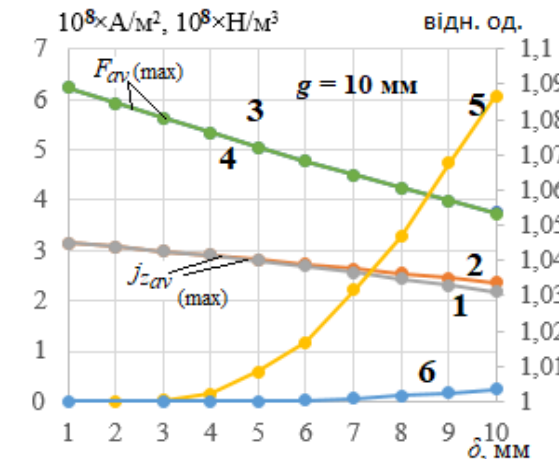


Fig. 7. Current and magnetic force on the depth of penetration of the electromagnetic field δ in accordance with the thickness of the plate $g=10$ mm.

In fig. 5... 6 it is seen that the current density in the presence and absence of a ferromagnetic platform begins to differ with the approach to $\delta \geq g$. Under the condition $\delta = g/2$ the current density with the presence of a ferromagnetic platform is 0.6..0.8% higher (curves 5 in fig. 6, 7). If $\delta = g$ - larger respectively on 1,2%, 5,5%, 8,7% (fig. 5, 6, 7). In case of equality $\delta = 10g$ (fig. 5) with the presence of a ferromagnetic platform, the current density is increased by 55%, and when $\delta = 2g$ (fig. 6) - respectively on 22%.

The magnetic force is almost the same with the ferromagnetic platform and without it in cases where the depth of permeability is not more than the thickness of the non-magnetic plate $\delta \leq g$ (fig. 5...7 - curves 6). If $\delta = 5g...10g$ (fig. 5), then the density of the magnetic force is lower using a ferromagnetic platform, respectively, by 2... 15%..

Conclusion

The performed studies of the model of the induction system with a U-shaped magnetic circuit and a ferromagnetic platform are relevant for the case when the ferromagnetic platform is not saturated. Thus, it is shown to what maximum values and under what conditions it is possible to strive to increase the current density and magnetic forces in welded joints of non-magnetic plates using a ferromagnetic platform with minimal saturation.

It is established that the presence of a ferromagnetic platform, other things being equal, allows to increase the current density in the weld to 55% if the depth of penetration of the electromagnetic field is greater than the thickness of the nonmagnetic plate 10 times, and up to 8% if the depth of field penetration is equal to the plate thickness.

The current density in the weld of the machined plate with a thickness of 1, 5 and 10 mm is greater in the presence of a ferromagnetic platform by 1.2, 5.5 and 8.7%, provided that the depth of penetration of the magnetic field is equal to the thickness of this plate. The magnetic force in the weld is less by 2... 15% with the presence of a ferromagnetic platform, if the depth of penetration of the electromagnetic field is greater than the thickness of the non-magnetic plate, respectively, 5... 10 times.

At the moment of opening of an electric circuit repeated increase of current density in a weld of a nonmagnetic plate can have on 50... 100% less value with presence of a ferromagnetic platform provided that depth of penetration of an electromagnetic field into a nonmagnetic plate in 1... 2 times exceeds thickness of this plate.

Authors: Andrii Bereziuk, candidate of technical sciences, docent of Department of Electrical Engineering, Electromechanics and Electrotechnology, National University of Life and Environmental Sciences of Ukraine, Geroev Oboroni str., 15, Kyiv, 03041, Ukraine, E-mail: marshall241987@gmail.com; Oleksiy Karlov, candidate of technical sciences, senior researcher of the Department of Electromagnetic Systems of the Institute of Electrodynamics of the NAS of Ukraine, prospekt Peremogy, 56, Kiev, 03680, Ukraine, E-mail: lexa.k.ua@gmail.com; Roman Kryshchuk, candidate of technical sciences, researcher of the Department of Electromagnetic Systems of the Institute of Electrodynamics of the NAS of Ukraine, prospekt Peremogy, 56, Kiev, 03680, Ukraine, E-mail: kr@nas.gov.ua; Ihor Garasymchuk, candidate of technical sciences, Head of Department of Electrical Engineering, Electromechanics and Electrotechnologies, Educational and Scientific Institute of Energy, Higher educational institution «Podillia State University», Shevchenko Str, 13, Kamianets-Podilskyi, 32316, Ukraine, E-mail: igorgarasymchuk@gmail.com; Pavlo Potapyskyi, candidate of

technical sciences, docent of Department of Electrical Engineering, Electromechanics and Electrotechnologies, Educational and Scientific Institute of Energy, Higher educational institution «Podillia State University», Shevchenko Str, 13, Kamianets-Podilskyi, 32316, Ukraine, E-mail: p.v.potap@meta.ua; Mykola Vusatyi, assistant of Department of Electrical Engineering, Electromechanics and Electrotechnologies, Educational and Scientific Institute of Energy, Higher educational institution «Podillia State University», Shevchenko Str, 13, Kamianets-Podilskyi, 32316, Ukraine, E-mail: 0611142015vys@gmail.com.

REFERENCES

- [1] Kuznetsov N, The influence of electric and magnetic pulse impact on the workpiece // Processing of materials by pressure, 2010, Vol. 3 (24), pp 126-129.
- [2] Komshina A, Pomelnikova A, Prospects of the method of low-energy processing of materials using a magnetic field // Science and Education. 2012, No. FS77 – 48211. pp. 463-488.
- [3] Lobanov M, Kondratenko I, Mykhalskyi V, et al. Electrotechnical complex for electrodynamic processing of welded joints // Technical electrodynamics, 2020, Vol 8, pp. 61-68.
- [4] Andrea D, Burleta T, Körkemeyerb F, et al. Investigation of the electroplastic effect using nanoindentation // Materials & Design, 2019, Vol 183, No. 108153.
- [5] Troitsky O, Stashenko V, Advantages of drawing and rolling metals with pulse current // IOP Conf. Series: Materials Science and Engineering, 2020, Vol. 848, No. 012084.
- [6] Vasetskyi Y, Kondratenko I. Electromagnetic field of inductors for local electric impulse impact on metal products // Technical electrodynamics, 2020. Vol. 4. pp. 11-14.
- [7] Kryshchuk R, Influence of winding ends on the parameters of pulse inductor with U-shaped core // Technical electrodynamics, 2020. Vol. 6. pp. 69-76.
- [8] Rashchepkin A, Kondratenko I, Karlov O, Kryshchuk R, Magnetic forces and inductor currents for magnetic pulse processing of welded joints of non-magnetic thin-walled metals // Technical electrodynamics, 2020. Vol. 5. pp. 74-79.
- [9] Rashchepkin A, Kondratenko I, Karlov O, Kryshchuk R, The influence of the U-shaped magnetic conductor of a pulsed inductor with two coils on the eddy currents of thin-walled non-magnetic metals in the process of magnetic pulse processing // Collection of "Proceedings of the Institute of Electrodynamics of the National Academy of Sciences of Ukraine", 2021. Vol. 59. pp. 20-27.
- [10] Voldek A, Induction magneto-hydrodynamic machines with a liquid metal working body. Energy, 1970. 272 P.
- [11] Neuman L, Demirchyan K, Theoretical foundations of electrical engineering. Energy, 1970. Vol. 2, 407 P.
- [12] Tamm I, Basics of the theory of electricity. Textbook allowance for universities, 11th ed. and additional. "Fizmatlit", 2003. 616 P.
- [13] Bereziuk A, Karlov O, Kryshchuk R. et al. Energy parameters of induction heat generator with branched heat exchanger for production of environmentally friendly coolant // Przegląd Elektrotechniczny. 2021. Vol97(7). pp. 48–51.